UCID-21739

EMI Potential of Proposed 115-kV Line Near B-691

Victor R. Latorre
Donald M. Wythe

July 27, 1989

Price Code	Page Range
A01	Microfiche
Papercopy Prices	
A02	001–050
A03	051–100
A04	101–200
A05	201–300
A06	301–400
A07	401–500
A08	501–600
A09	601

EMI POTENTIAL OF PROPOSED 115KV LINE NEAR B-691

by

Victor R. Latorre and Donald M. Wythe

Engineering Research Division
Electronics Engineering
Lawrence Livermore National Laboratory
Livermore, CA 94550

Introduction/Background

The Laser Operated Diamond Turning Machine (LODTM) is housed in Building 691. This facility contains electronic measurement and control systems which could be susceptible to interfering electronmagnetic interference (EMI) generated by sources external to B-691. In particular, concern has been expressed [1] that such harmful EMI signals could be produced by the proposed WAPA 115KV feeder line which would be routed approximately 30 feet from the East side of the facility. Also, there has been some concern expressed about the effects of the resulting electromagnetic (EM) fields on personnel in the proximity of the power line. Since it is necessary to measure the EM fields to ascertain if a hazard does indeed exist, and since we in ERD have been performing such field measurements for many years, we were contacted to determine the field levels from the line that might be expected inside and close to B-691. This report describes our approach, equipment and calibration procedures, analysis techniques used, results, and suggestions for future work in related areas.

Approach

In order to obtain bounds on the EMI levels that might be expected in and around B-691, we performed the following tasks:

1. A brief literature search on EM fields radiated from transmission lines.

2. Measurements of EM fields currently existing within and near B-691.

3. Measurements of EM fields from an isolated 115KV transmission line.

4. Measurements of EM fields in close proximity to a multi-line station within LLNL.

Noise Sources on Transmission Lines

From the literature [2-8], it is clear that there are two sources of EMI radiated by transmission lines. The first is corona which is distributed along the power line conductor and tower hardware. Below about 30 MHz,the amplitude of the noise spectrum is inversely proportional to the square of the frequency, while above 30 MHz, it appears to be proportional to the inverse of the frequency [3]. The second EMI source is spark and microspark discharges between gaps on the transmission line hardware. The spectrum of this noise contains more high frequency components than corona noise, and its amplitude is also inversely proportional to frequency above 30 MHz. It is interesting to note that corona noise has been observed at frequencies up to 900 MHz, while gap noise has been detected up to 8 GHz [6].

Corona noise from conductors is the dominant noise below 30MHz, while gap noise usually predominates above that frequency in fair weather. This is particulary true for lower voltage lines because they have less corona activity. In foul weather, however, gap sources can be shorted by water and corona activity from conductor and hardware increases under these conditions. Thus, corona noise dominates in foul weather, and is more pronounced for higher voltage lines. This corona noise is caused mainly by surface perturbations on the line and tower structure formed by water and insects. These cause local increases in the electric field and resulting breakdown of nearby air molecules, and can be modeled as small electric dipoles [7]. In reference [7], a dipole model was used to determine the electric field from a 1200KV line of 35.5m outside height, and resulted in a maximum field strength of approximately 0.3 v/m at 75 MHz. This value compared closely with their experimental results during a rain storm, and gives us an approximate idea of field levels found by others.

EMI Field Measurements

Although the EM field values taken from our small sampling of the literature indicate rather modest field strengths caused by corona on transmission lines, we felt it was necessary to perform actual site measurements ourselves. As indicated earlier, our approach involved determining existing fields within critical areas of the LODTM facility, and then measuring the fields created by transmissions lines over the same frequency range (100 Hz to 1.5 GHz). In this way, we felt that we could bound the problem by comparing existing EM fields within and around B-691 with those caused by a relatively isolated 115KV line (crossing the Sandia parking lot) and a multiple high voltage transmission line configuration existing next to the switch yard outside of B-424.

The measurements were made with a variety of antennas, active and passive, which drove a Hewlett-Packard model 8568A spectrum analyzer and/or a Tecktronics model 7854 oscilloscope. The oscilloscope was used merely to obtain a "feel" for the EM environment; the actual quantitative data were obtained using the spectrum analyzer and recorded with a Polaroid camera. We were therefore able to obtain real-time data and, by using the "Peak Hold" feature of the spectrum Analyzer, a time-integrated record of both transient and steady EM signals present.

Before proceeding to a discussion of the results of our measurements, we first describe the equipment, calibration procedures, and analysis techniques used on this brief task. It is important to do this so that you will know exactly how the data were obtained, and how we obtained our quantitative results.

Equipment and Calibration

In the previous section, we mentioned the equipment used in the task. Since the oscilloscope was used only to obtain an idea of the real-time EM fields present, and a Polaroid camera is a Polaroid camera, further discussion of these two pieces of equipment will not be pursued here. We will, however, provide some details on the operating ranges and characteristics of the spectrum analyzer and antennas used.

The spectrum analyzer used in this task is a Hewlett-Packard (HP) model 8568A, which operates from 100 Hz to 1.5 GHz. It has a dynamic range of over 100 dBm, so that it is easily capable of operating down past the "noise floor" in our applications. Since all spectrum analyzers are power devices, they provide data in dBm (dB above a milliwatt). Because we desire to know input voltages from our antennas, it is necessary to convert the power

readings on the spectrum analyzer to voltages. This is easily accomplished because the input impedance of the spectrum analyzer is a resistive 50 Ohms. An illustration of the conversion procedure is presented in a later section.

It is particularly important to know the actual response of the antennas. This is necessary because the voltage from the antenna to the spectrum analyzer must be related to the electric or magnetic field in order to quantify the fields in which the antennas are immersed. The antenna characteristic that provides this information is the antenna factor, AFE, which is defined as the ratio of the electric field intensity (E) to the output voltage of the antenna into a matched load. How we find AFE (the calibration procedure for an antenna) is described below.

Our antennas are calibrated in a TEM (Transverse Electric and Magnetic) cell. A diagram of this facility, along with a HP automatic network analyzer (ANA), is shown in Figure 1. The system is first calibrated (the effects of the antenna's physical presence and the connecting cables are nulled-out) by connecting the output of the TEM cell to the ANA's input, and performing the calibration automatically. For the actual measurement of the antenna factor, the input to the ANA is now switched to the antenna output, the TEM cell output terminated in a 50-Ohm load, and the subsequent frequency characteristic plotted. This procedure is followed for all antennas used in our field measurement programs.

It is important to note, however, that the TEM cell we have will only provide accurate results up to approximately 100 MHz. The reason for this is that above 100 MHz, other modes in addition to the TEM mode start to appear in the cell. These modes will interfere with the principal one (TEM), and the subsequent antenna responses are therefore not quantifiable. It may be argued that the cell could be made smaller to preclude higher order modes from appearing at such a low frequency; however, if this were to be done , the working volume within the cell would be decreased proportionally. Thus, we see the dilemma faced by TEM cell designers and manufacturers - the trade-off between working volume and cut-off frequency. At any rate, for purposes of this task, the cell is more than adequate.

There is one other factor that must be considered when finding the antenna factor from measurements made within a TEM cell. During the actual calibration, the electromagnetic wave travels the entire length of the cell, while, during the actual measurement, the wave only travels down a portion of it - usually about one half. Thus, there will be a phase shift associated with the data (about comparable to a 4 nanosecond time delay). This shift will not influence the amplitude portion of the response, which, for the work described

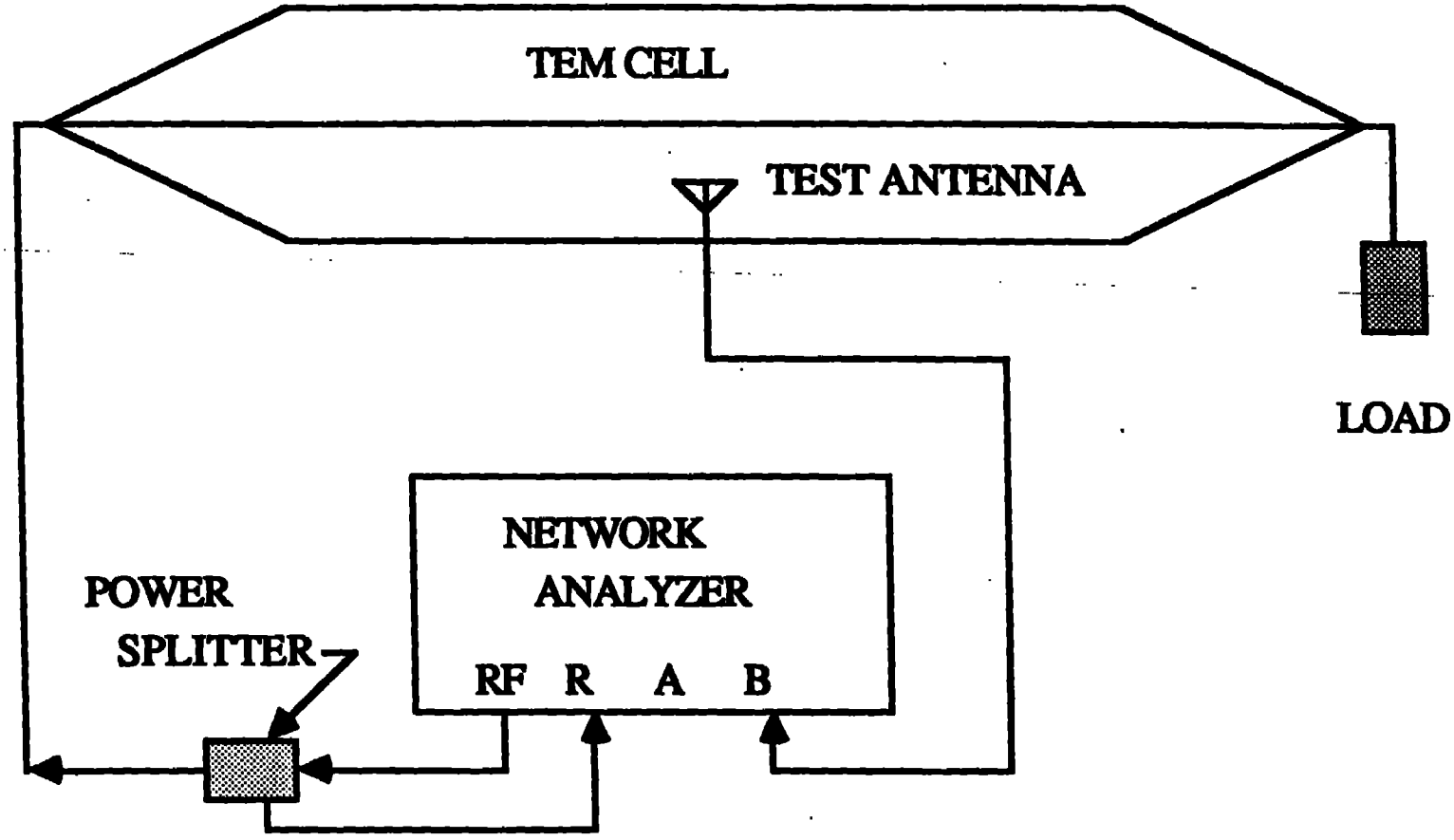

FIGURE 1. ANTENNA CALIBRATION CONFIGURATION

in this report, is all we are interested in at this time. If we were concerned about phase for some other applications, we would, therefore, have to compensate for the different path lengths used in calibration and measurement.

Figures 2, 3, and 4 are plots of the responses of the MGL-S5B(R) B-Dot, LLNL Active, and the ARA SAS 1/D active antennas. There are two bands shown in each figure for each antenna. The highest values of the fields occurred at or below 40 MHz, and we wanted to concentrate on this portion of the EM spectrum after first checking to see that this was indeed the region in which the maximum fields were encountered. Thus, two plots for each antenna are provided. In addition, we have provided the response plot of the SAS active antenna, Fig. 5, since it is the one we used for the majority of our measurements above about 100 MHz. Since the manufacturer's characteistics for this antenna agreed closely with our TEM cell measurements of the antenna up to 94 MHz, we felt we could have confidence in its higher frequency response.

Analysis Techniques

From the brief description of the spectrum analyzer provided above, it was mentioned that the values displayed on the analyzer's screen are given in dBm - decibels above a milliwatt. It's input impedance was also given as 50 Ohms. To use the antenna factor to obtain the field, the voltage input to the analyzer must be found. This is done as follows:

1. Take the signal value in dBm and convert to Watts by using

$$mW = 10^{dBm/10}, \tag{1}$$

$$W = mW \times 10^{-3} \tag{2}$$

2. Convert the signal value in Watts to voltage across the 50-Ohm input by using

$$v = (W \times 50)^{1/2} \tag{3}$$

3. Express the peak voltage in terms of the measured power (in dBm) by

$$v_p = \frac{(10^{dBm/10} \times 10^{-3} \times 50)^{1/2}}{\sqrt{2}} \tag{4}$$

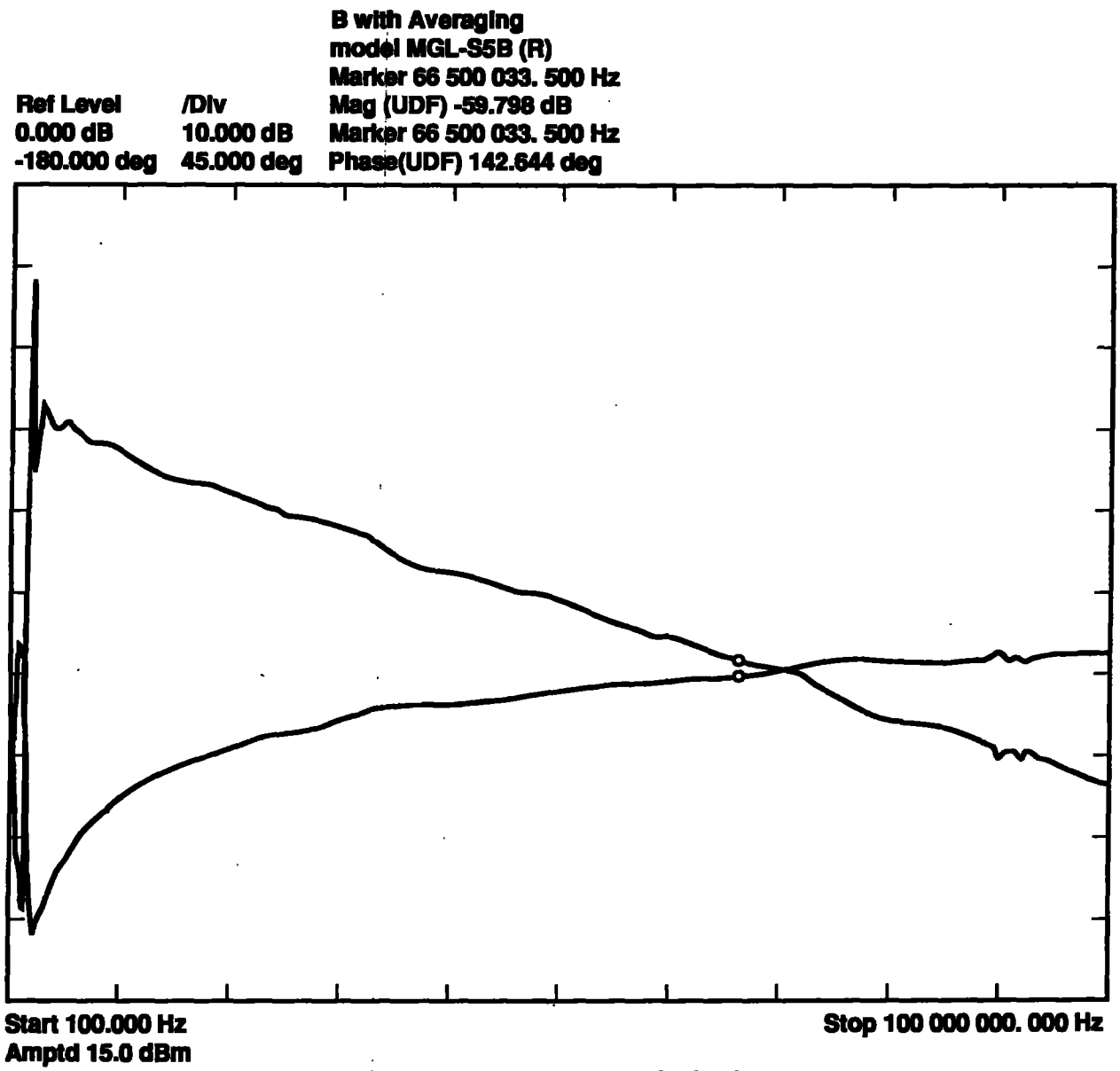

Fig. 2 B-dot response in TEM cell

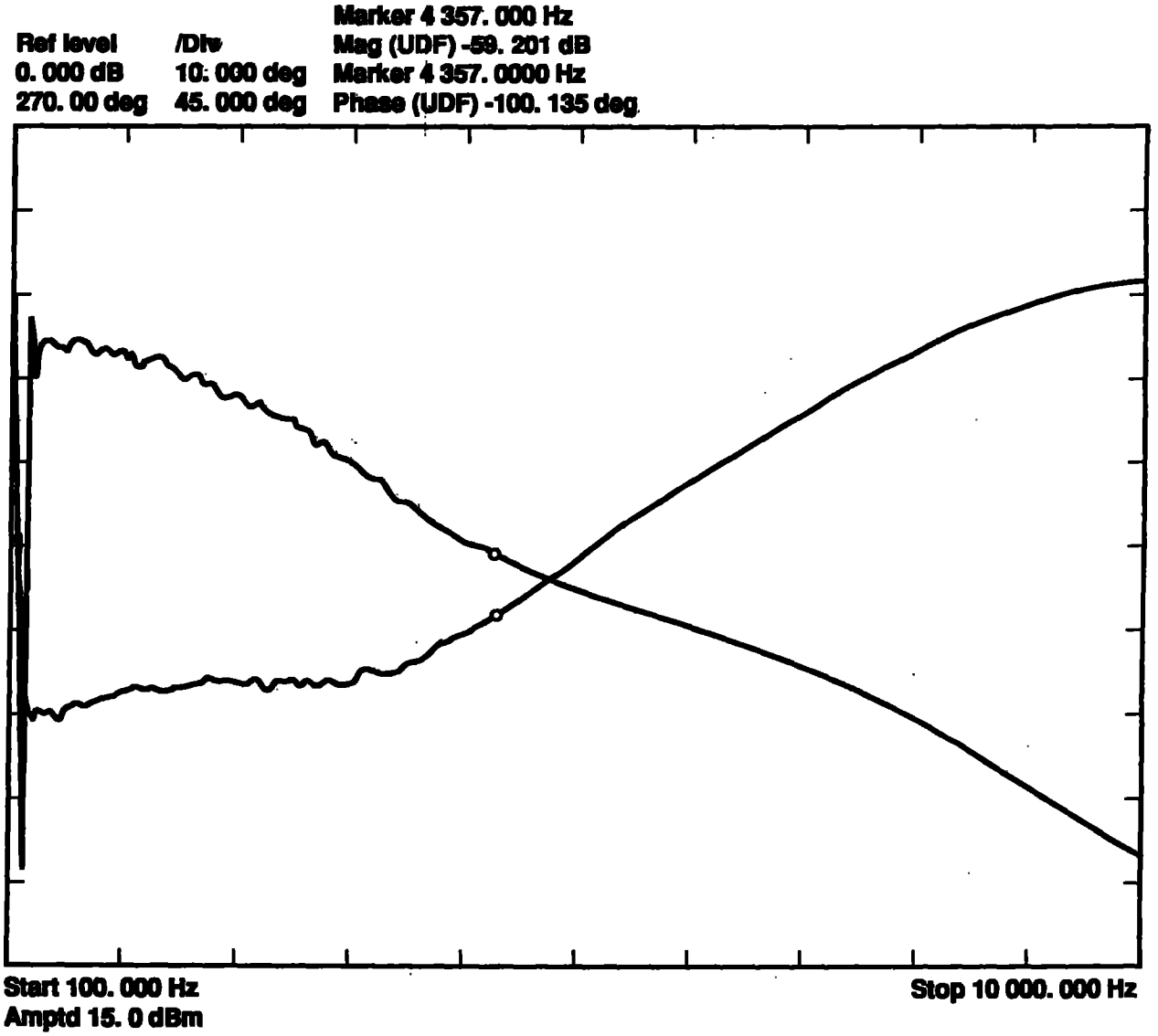

Fig. 3a LLNL active response in TEM cell (Lo)

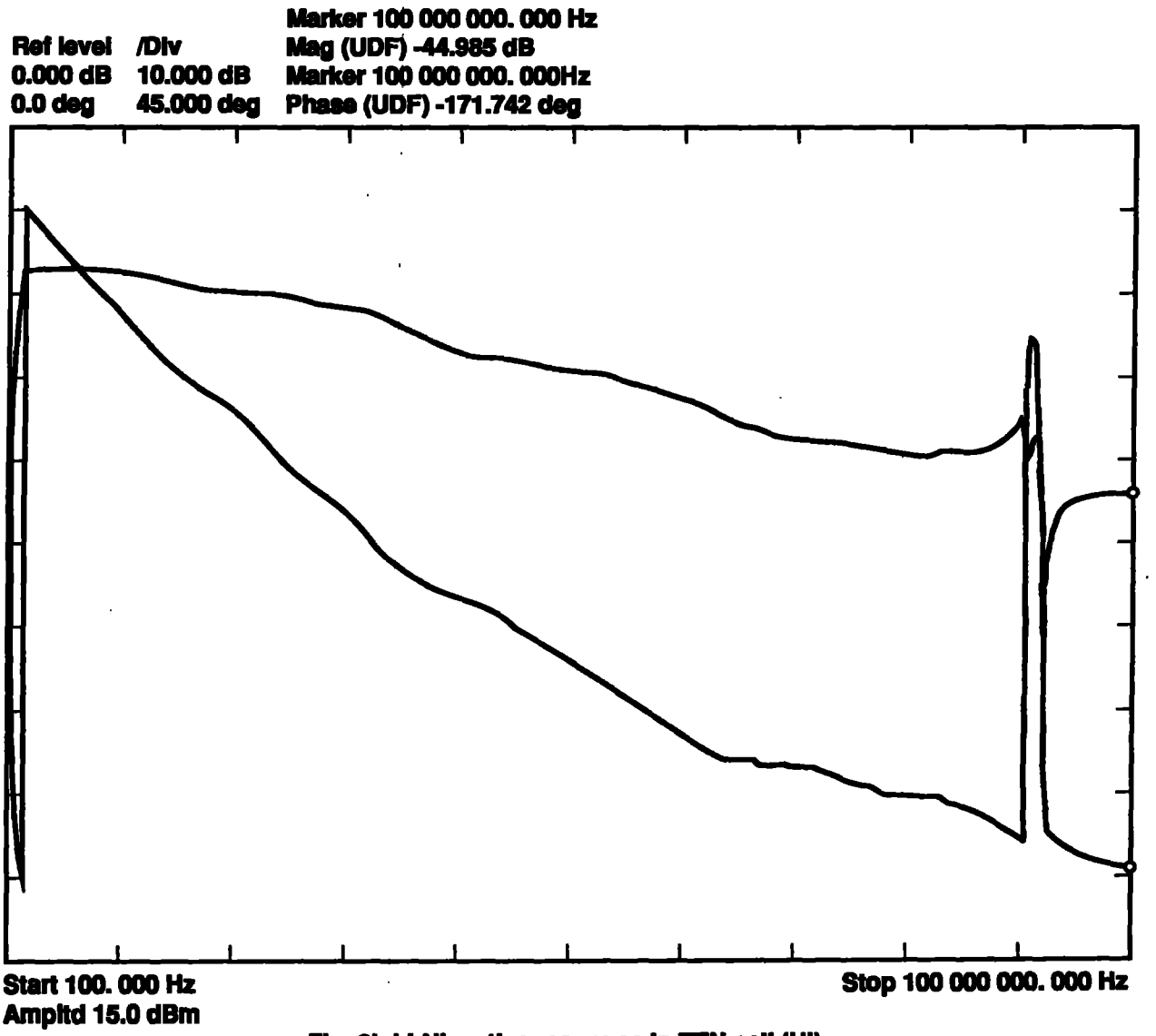

Fig. 3b LLNL active response in TEN cell (HI)

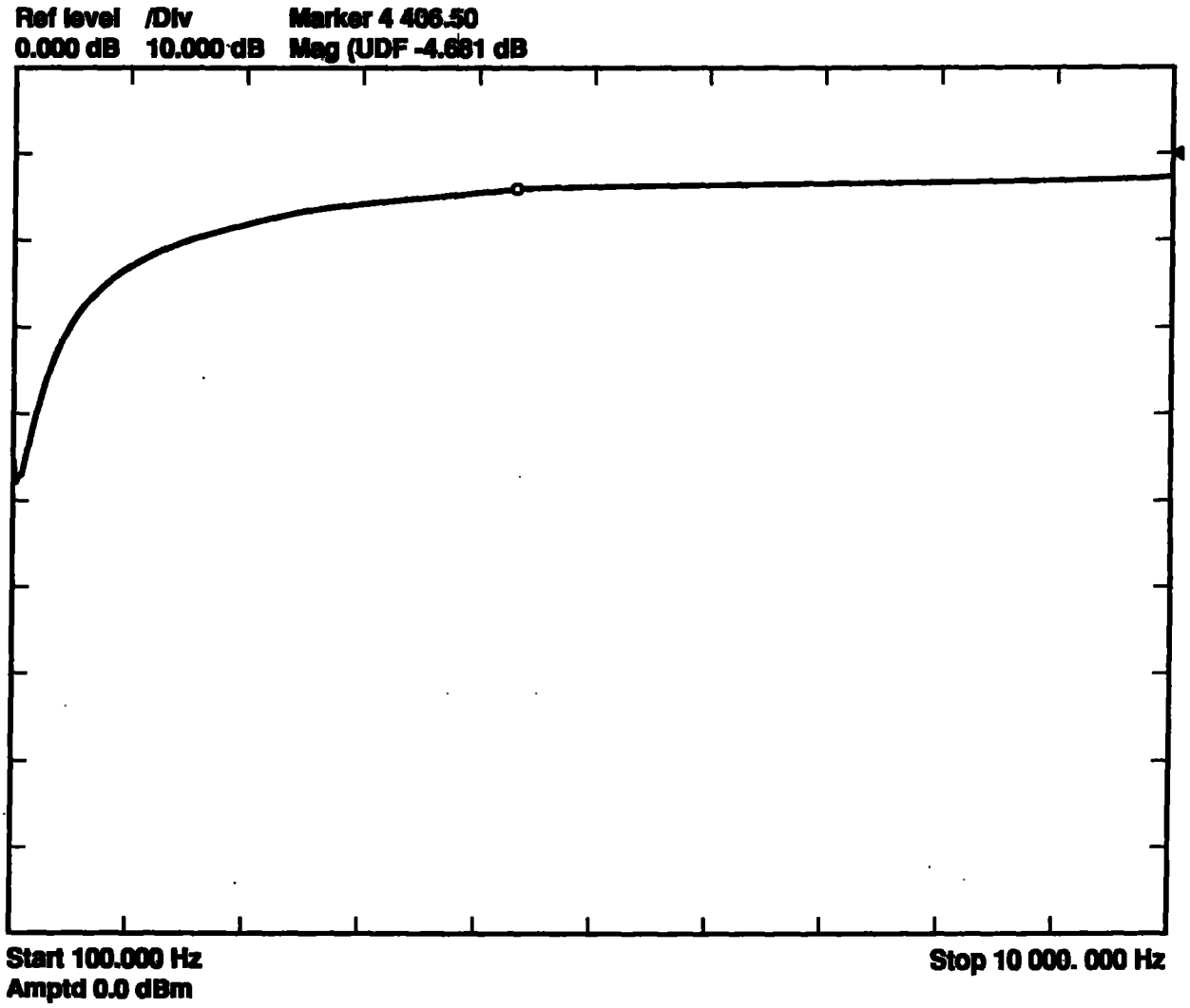

Fig. 4a SAS antenna response in TE

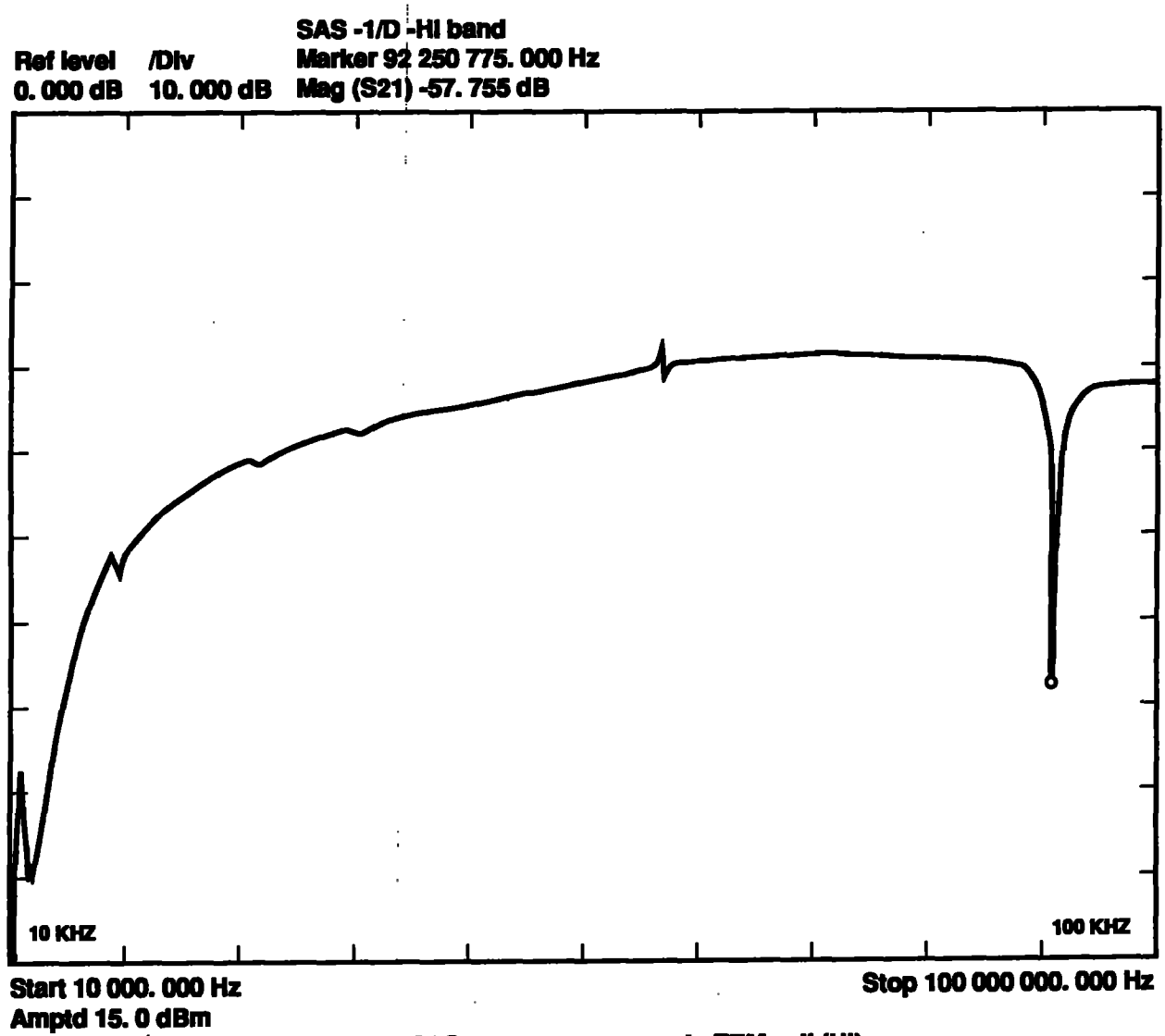

Fig. 4b SAS antenna response in TEM cell (HI)

We now have the peak value of the voltage developed by the linear antenna across the input terminals of the spectrum analyzer. This value, taken with the antenna factor or the effective area of a B-dot probe will now give the value of the electric or magnetic field which the antenna is receiving.

There are still some complications, however, when using B-dot or D-dot probes, which, as their names imply, provide the time derivative of either the magnetic or electric field. In addition, we must also know the effective area of each probe if we are to determine the overall antenna response of such a device. The procedure here is best illustrated by the actual calculation of peak magnetic field intensity as measured by one of the probes (antennas) used on the task. Following that section, the determination of the peak electric field intensity will then be presented.

Calculation Of Peak Magnetic Field Measured By A B-Dot Probe

Magnetic fields are measured with a B-Dot ($\dot{B}$) probe, which produces an output voltage given be

$$v = \dot{B} A_{eff}, \tag{5}$$

or

$$\dot{B} = v/A_{eff}, \tag{6}$$

where

$\dot{B}$ = time derivative of the magnetic induction (= uH, with H defined as the magnetic field intensity, and u the permeability of free space)

A_{eff} = the effective area of the antenna (probe)

Performing the integration of equation (5),

$$B = v_p \sin(wt)/wA_{eff}, \tag{7}$$

and, therefore, the peak value of the magnetic field intensity becomes

$$H_p = v_p/uwA_{eff} \tag{8}$$

The value of the peak voltage (for sinusoidal functions) is 1.414 times the r.m.s. voltage, v_{rms}, which is what we must use when converting the power indicated by the spectrum analyzer to voltage. This conversion was done previously and is provided by equation (4). Thus, combining equations (4) and (8), we have

$$H_p = \frac{(10^{dBm/10} \times 10^{-3} \times 50)^{1/2}}{uwA_{eff}} \qquad (9)$$

From our measurements, the peak value of the magnetic field occurred at 40 mHz, and had a value of -25 dBm. The effective area of the B-dot probe is 0.001 square meter, and the value of u is $4\pi \times 10^{-7}$. Using these values in equation (9), we find the peak magnetic field in the facility to be 0.04 Amperes per meter.

Calculation Of Peak Electric Field Measured By LLNL Active Antenna

The antenna factor for the SAS active antenna was determined to be 10 at 40 MHz, the frequency of the highest electric field component present in the pit of the facility. The value of the power developed by this electric field as read by the spectrum analyzer was -15 dBm. By combining the definition of AFE with equation (4), the expression for the peak electric field is

$$E_p = 1.414 \times AFE \ (10^{-3} + dBm/10 \times 50)^{1/2} \qquad (10)$$

Thus, using the above measured value for AFE and the value of power in dBm as measured by the spectrum analyzer, the peak electric field intensity in the pit is found to be 0.18 volts per meter.

Experimental Results Inside B-691

By following the procedure summarized above, we were able to identify such EM sources as Radio Pagers, Commercial Broadcast stations, and similar entities that contribute to the overall EM spectrum. In addition, we were able to correlate some of the responses to equipment within the facility itself. Some of these sources were identified as follows:

1. 40 MHz Laser

2. 45 MHz Laser Driver
3. 65 MHz Laser
4. 80 MHz Laser Driver - Second Harmonic
5. 101 MHz FM Radio
6. 106.8 MHz FM Radio
7. 120 MHz Laser Driver - Third Harmonic
8. 146.2 MHz Ham Radio
9. 164 MHz LLNL Police
10. 263 MHz Aircraft
11. 411 MHz LLNL Pager System
12. 604 MHz Channel 36 (TV)
13. 641 MHz Channel 42 (TV)
14. 770 MHz Channel 64 (TV)
15. 880 MHz Cellular Telephone
16. 930 MHz Cellular Telephone

The measurements were made in five locations within the facility, and the resulting spectra are presented in Appendix A. The locations monitored and the corresponding data are:

1. Turning Room Figures 1 - 7; Figures 11 - 13.

2. Control Room Figures 8 - 10.

3. Pit Figures 14 - 19.

4. Pump Room Figures 20 - 23.

5. Vacuum Room Figures 24 - 27.

As shown by the oscilloscope photographs of the EM spectra existing within B-691 without the presence of the proposed 115KV transmission line, there is a considerable amount of electromagnetic energy present. The highest values are to be found in the pit, right next to the lasers, while the lowest overall EM values were found to exist in the Pump Room. Apparently, the presence of these signals have not caused significant problems within the building. If they have, we would recommend shielding the primary offenders - the lasers and drivers.

EM Radiation From An Isolated 115KV Transmission Line

The second series of measurements was performed in the West Parking Lot of the Sandia Corporation in Livermore. The source was a 115KV transmission line running North-South across the lot at a height of about 20 meters. Since there are no other transmission lines in the immediate area, this line provided us with a good opportunity to determine EM fields essentially radiated solely by that source (with the exception of radio stations, etc.). From the results, shown in Figures 28 - 32 in Appendix A, it can be seen that the highest field levels result from commercial radio stations and the LLNL Police radio. We were simply not able to see major EM components that we could attribute to the line itself, particularly in the 1 MHz to 300 MHz range, which is the frequency band of primary interest to the LODTM personnel. It is also noted that the measurements were performed during a light rain, a condition which, from what we have found in the literature, constitutes the worst environment with respect to corona noise.

EMI Radiation From A Switching Station

In order to determine an upper bound on EM radiation from power transmission lines, we set-up our measurement apparatus next to an on-site switching station near B-424 at LLNL. The reasons for selecting this location was the low physical height of the power lines, the multiplicity of lines, transformers, insulators, and associated switch gear, which should all contribute to the corona noise. In addition, the measurements were performed in a light rain.

The results of the measurements are presented in Figures 33 - 36. Neglecting the commercial radio and LLNL Police emissions, the overall EM field levels are slightly greater than those observed from the "isolated" 115KV line, but are still not high, particularly throughout the 1 to 300 MHz range.

EMI Radiation Measurements Outside of B-691

Our final series of EMI measurements was made outside of the LODTM facility. The location of our antennas was again in the area of maximum field strengths - in this case, just to the South East of the larger loading doors. The results of the measurements are presented in Figures 37 - 41 in Appendix A. Once again, the largest signals were caused by commercial and local Police radios, although we did observe some lower frequency EMI from the building itself.

Results And Conclusions

The maximum electric and magnetic field were observed to occur in the Pit of B-691, and were both at 40 MHz. They were, respectively, 0.178 v/m and 0.055 A/m. These fields were considerably greater than any fields generated by the high voltage transmission lines as measured in a light rain. The 40 MHz fields and their harmonics are attributable to the laser system itself, as were other relatively prominent fields at 45 and 65 MHz. The 164 MHz LLNL Police signal was also observed to be prominent throughout the LODTM facility. It is recommended that the sources internal to the facility be shielded if there is concern about their potential to interfere with critical electronic systems comprising the LODTM and related systems.

As far as the signal from the LLNL Police is concerned, equipment that may be affected could be shielded as well. It is important to note that, in general, the most serious threat to electronic systems is posed by penetrators; that is, conductors that may couple unwanted signals into sensitive systems. Thus, it is necessary to employ correct grounding and shielding techniques to mitigate these effects.

For all signals detected during our measurements, none were found to constitute a hazard to personnel. This conclusion is based on the guidelines set forth in the LLNL Health and Safety Manual for Radiofrequency/Microwave Radiation and Fields [9].

It must be remembered that we did not investigate any signals lower in frequency than 100 Hz. However, since the primary concerns with the electronic susceptibility were with the 10 MHz through 300 MHz region of the EM spectrum, we feel our comments on the equipment are valid.

Future Work

Because of the relatively low-level fields we measured from the transmission lines, it is apparent that they and their accociated hardware are quite clean. It might be prudent, however, to establish a periodic measurement program that might detect an intolerable increase in corona or gap noise from the high voltage transmissions systems. Also, a similar program to periodically monitor fields within the LODTM facility may be useful as well.

REFERENCES

1. Stowers, I. F., and S. R. Patterson, Memorandum PEP 89-13, February 13, 1989.

2. Warburton, F. W. et al, "Power Line Radiations and Interference Above 15 MHz", IEEE Trans. on Power Applications and Systems, Vol. PAS-88, No. 10, Oct. 1969.

3. Pakala, W. E. and V. L. Chartier, "Radio Noise Measurements On Overhead Power Lines From 2.4 to 800 KV", IEEE Summer Power Meeting, July, 1970.

4. Transmission Line Reference Book - 345 KV and Above, 2nd Edition, EPRI, Palo Alto, CA, 1982.

5. Arai, K. et al, "Micro-Gap Discharge Phenomena and Television Interference", IEEE Trans. on Power Applications and Systems, Vol. PAS-104, No. 1, January, 1985.

6. Chartier, V. L. et al, "Electromagnetic Interference Measurements at 900 MHz on 230 KV and 500 KV Transmission Lines", IEEE Trans. on Power Systems, Vol. PWRD-1, No. 2, April,1986.

7. Olsen, R. G. and B. O. Stimson, "Predicting VHF/UHF Electromagnetic Noise From Corona on Power-Line Conductors", IEEE Trans. on EMC, Vol. 30, No. 1, Feb. 1988.

8. Al-Arainy, A. A. et al. "Electromagnetic Interference From Transmission Lines Located in Central Region of Saudi Arabia, IEEE Trans. on Power Delivery, Vol. 4, No. 1, January, 1989.

9. Miller, Gordon, Health and Safety Manual, Supplement 23.57, Radiofrequency/Microwave Radiation and Fields, LLNL, May, 1988.

APPENDIX A

EMI MEASUREMENT DATA

FOR LODTM TASK

ABBREVIATIONS

D	Driver (Laser)
CR	Control Room
H	Horizontal Polarization
L	Laser
LLNLA	LLNL Active Antenna
Pit	Room Under Turntable
PR	Pump Room
SAS	Commercial Wideband Active Antenna
SL	Sandia Parking Lot
SY	LLNL Switch Yard
TR	Turning Room
V	Vertical Polarization
VCR	Vacuum Clean Room
691X	East Parking Lot of B-691

Ref. 0 dBm
Atten. 10 dB
Scale. 10 dB/Div.
Freq. 0-400 MHz

Fig. 1 TR-SAS (V), D on; L off

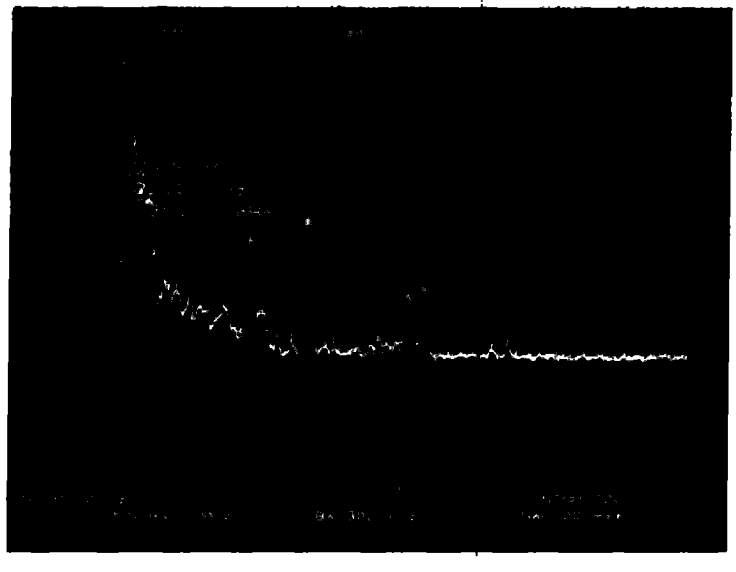

Ref. 0 dBm
Atten. 10 dB
Scale. 10 dB/Div.
Freq. 0-200 MHz

Fig. 2 TR-SAS (V), D on; L off

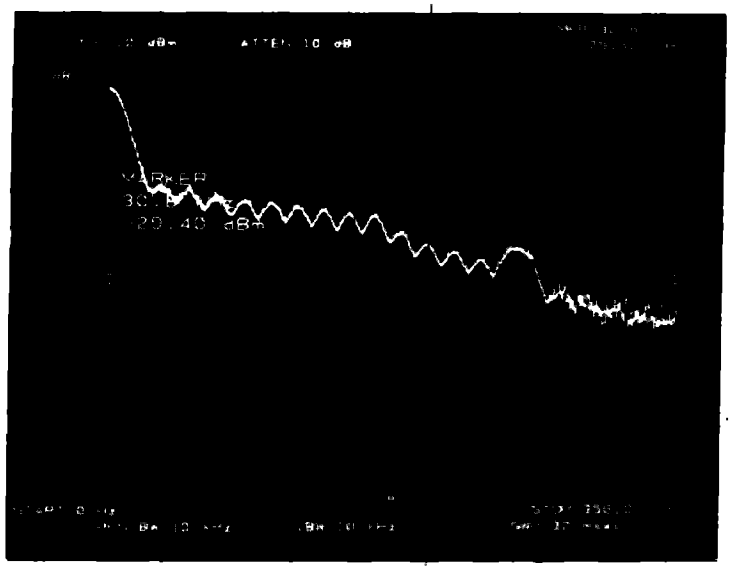

Ref. 0 dBm
Atten. 10 dB
Scale. 10 dB/Div.
Freq. 0-350 MHz

Fig. 3 TR-SAS (V), D on; L off

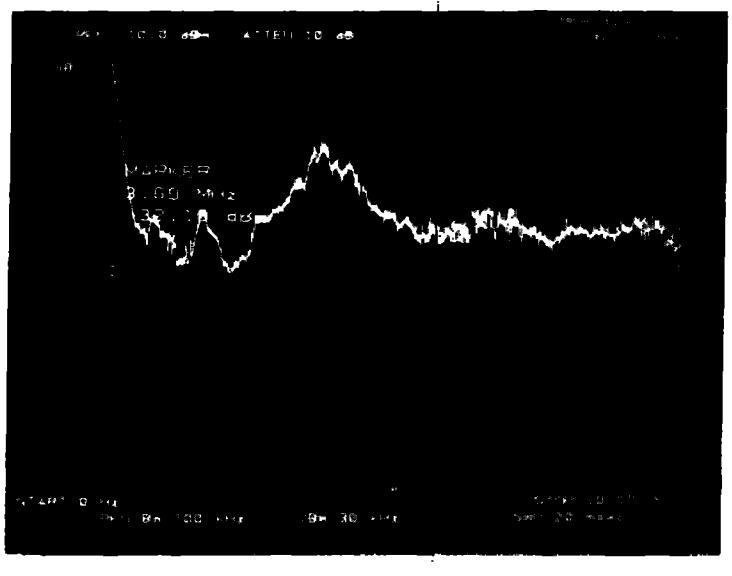

Ref. 0 dBm
Atten. 10 dB
Scale. 10 dB/Div.
Freq. 0-200 MHz

Fig. 4 TR-SAS (V), D on; L off

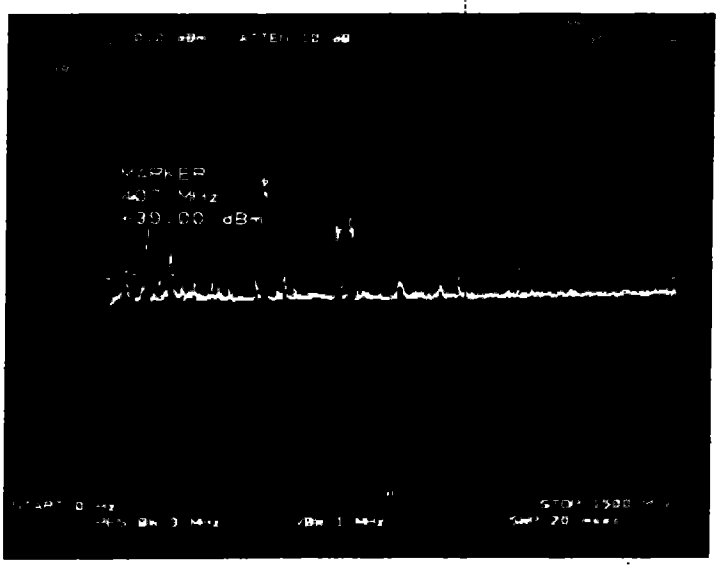

Ref. 0 dBm
Atten. 10 dB
Scale. 10 dB/Div.
Freq. 0-1500 MHz

Fig. 5 TR-SAS (V), D on; L off

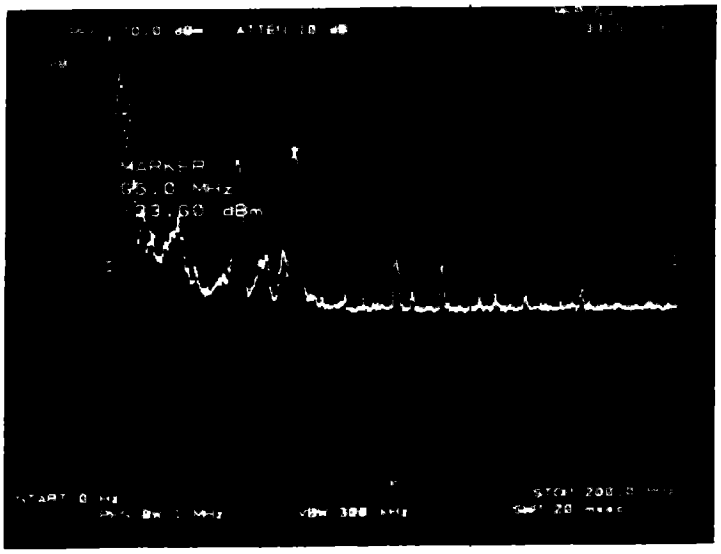

Ref. 0 dBm
Atten. 10 dB
Scale. 10 dB/Div.
Freq. 0-200 MHz

Fig. 6 TR-LLNLA (H), D on; L off

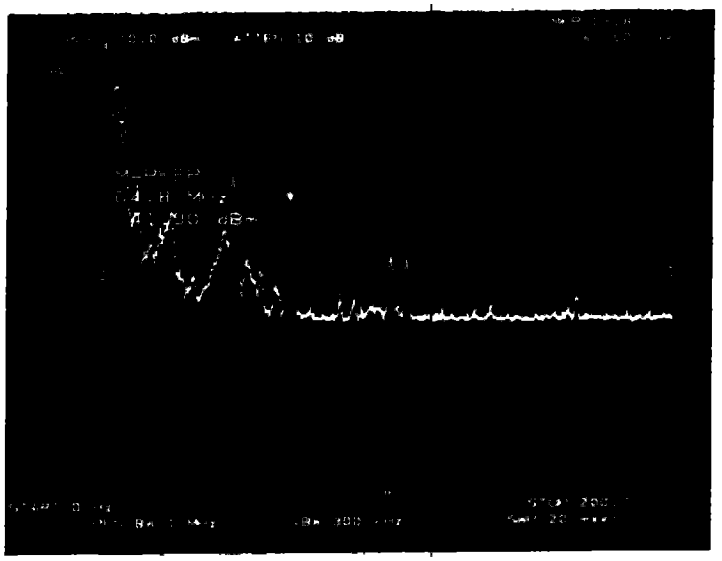

Ref. 0 dBm
Atten. 10 dB
Scale. 10 dB/Div.
Freq. 0-200 MHz

Fig. 7 TR-SAS (V), D on; L off

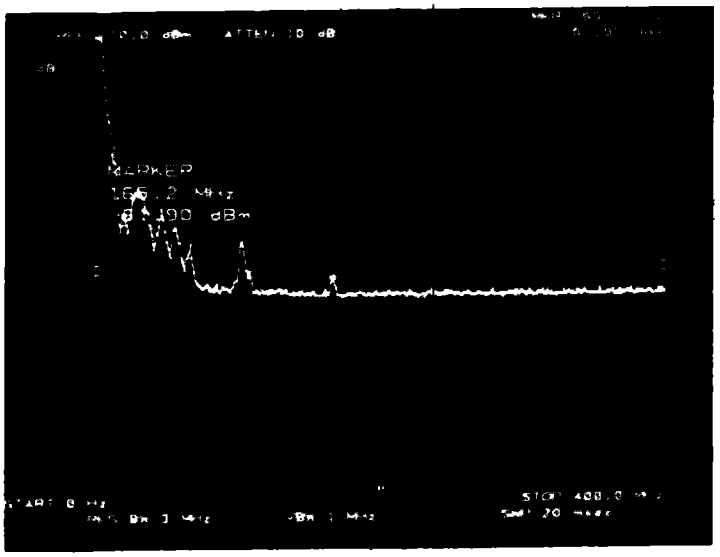

Ref. 0 dBm
Atten. 10 dB
Scale. 10 dB/Div.
Freq. 0-400 MHz

Fig. 8 CR-SAS (V), D on; L off

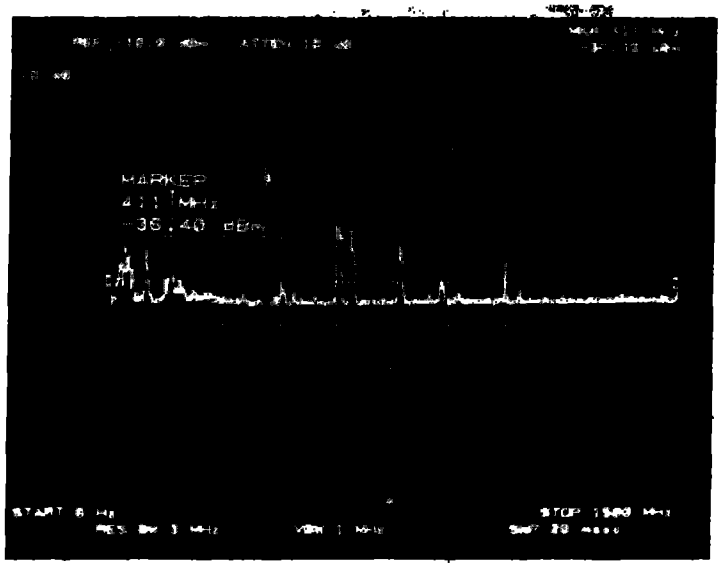

Ref. 0 dBm
Atten. 10 dB
Scale. 10 dB/Div.
Freq. 0-1500 MHz

Fig. 9 CR-SAS (V), D on; L off

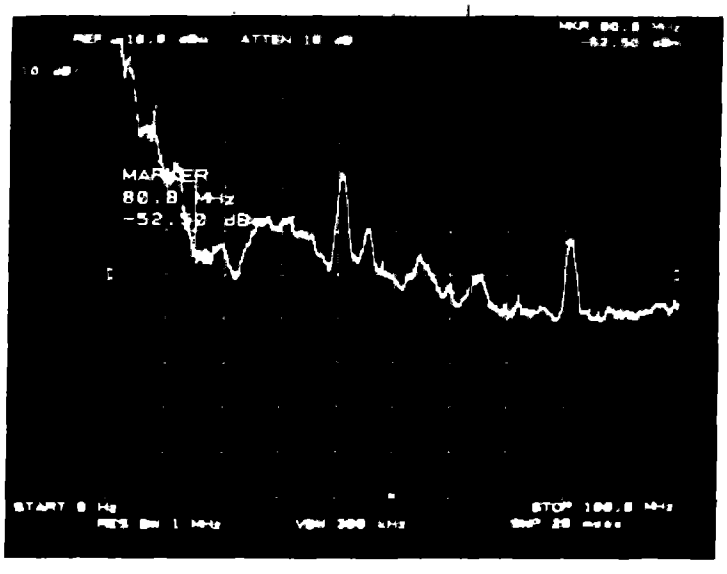

Ref. 0 dBm
Atten. 10 dB
Scale. 10 dB/Div.
Freq. 0-100 MHz

Fig. 10 CR-SAS (V), D on; L off

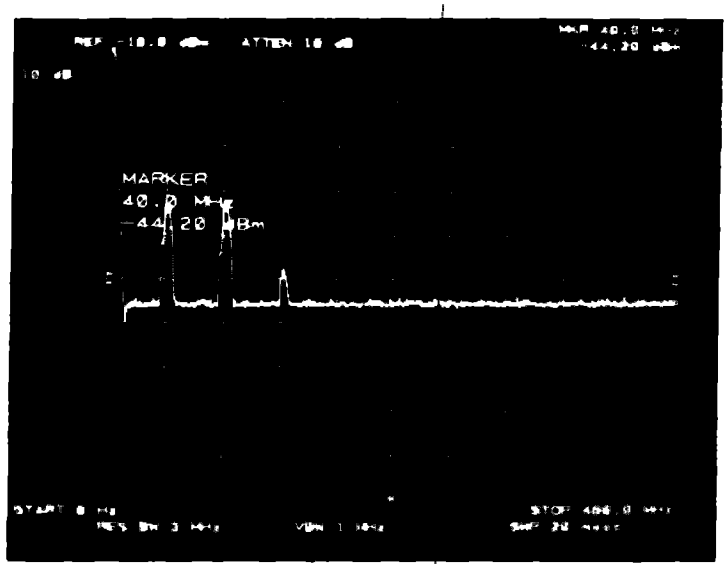

Ref. -10 dBm
Atten. 10 dB
Scale. 10 dB/Div.
Freq. 0-400 MHz

Fig. 11 TR-D-Dot, D on; L off

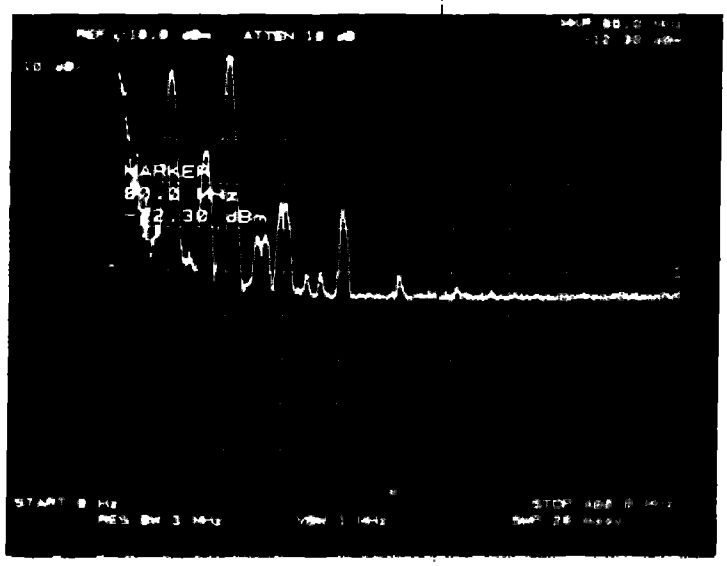

Ref. -10 dBm
Atten. 10 dB
Scale. 10 dB/Div.
Freq. 0-400 MHz

Fig. 12 TR-SAS (V), D, L on

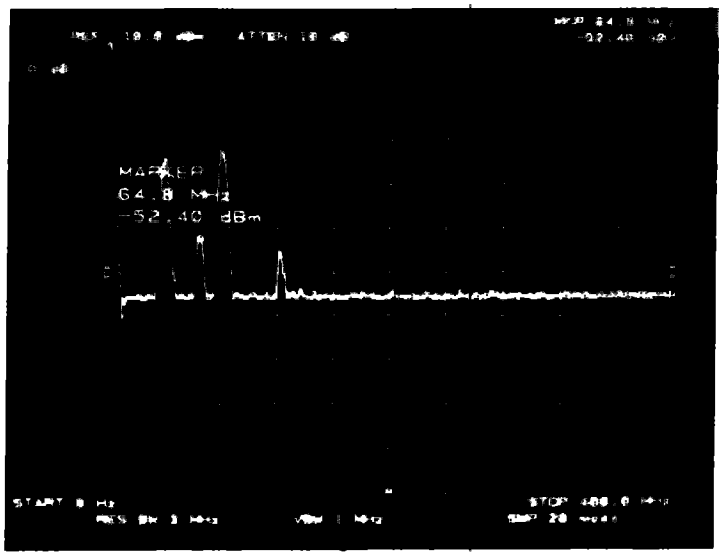

Ref. -10 dBm
Atten. 10 dB
Scale. 10 dB/Div.
Freq. 0-400 MHz

Fig. 13 TR Floor- D-Dot, L on

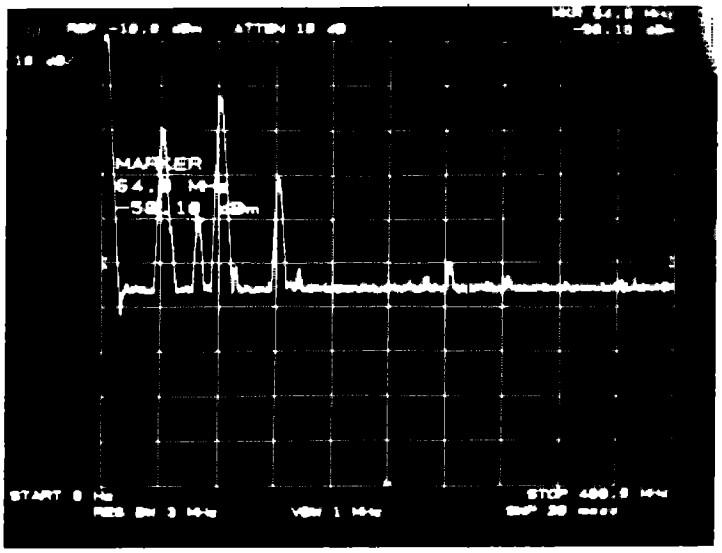

Ref. -10 dBm
Atten. 10 dB
Scale. 10 dB/Div.
Freq. 0-400 MHz

Fig. 14 Pit-D-Dot, D, L on

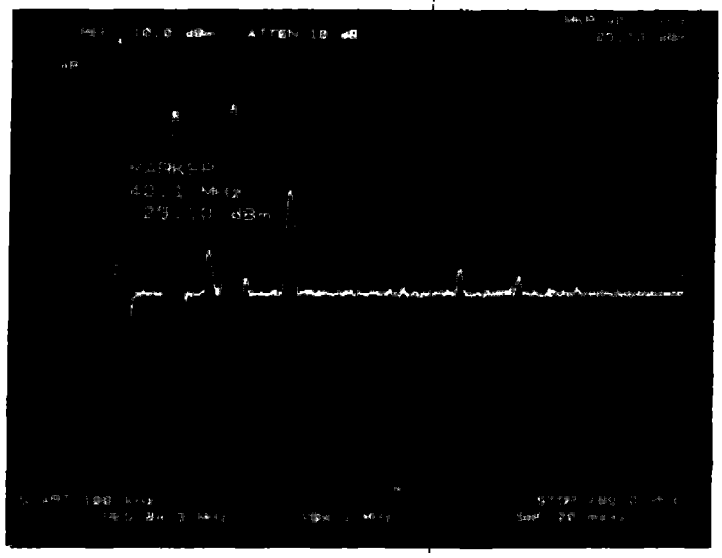

Ref. -10 dBm
Atten. 10 dB
Scale. 10 dB/Div.
Freq. 0-400 MHz

Fig. 15 Plt-B-Dot, D, L on

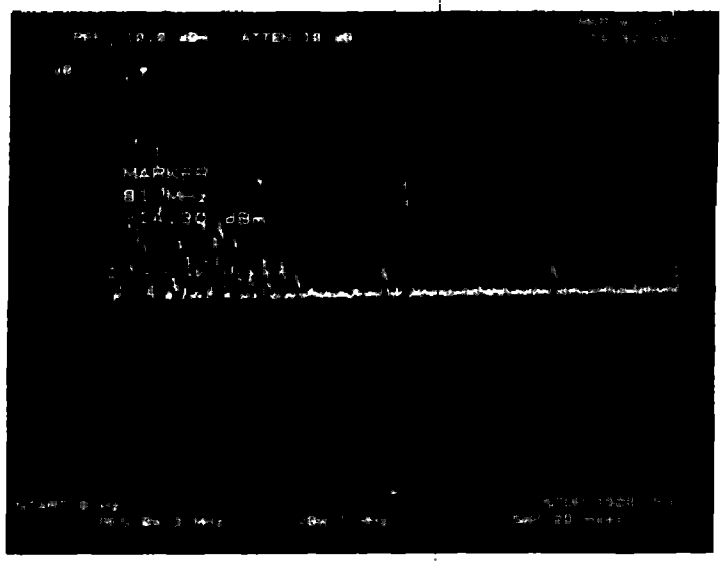

Ref. -10 dBm
Atten. 10 dB
Scale. 10 dB/Div.
Freq. 0-1500 MHz

Fig. 16 Plt-SAS (V), D, L on

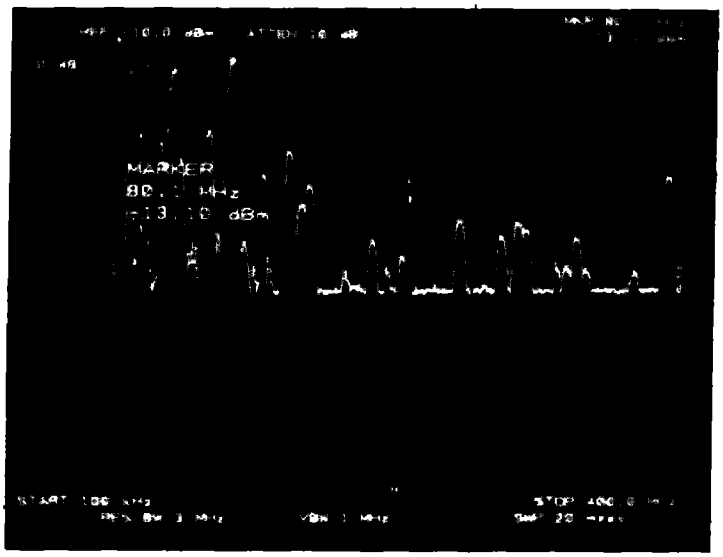

Ref. -10 dBm
Atten. 10 dB
Scale. 10 dB/Div.
Freq. 0.1-400 MHz

Fig. 17 Plt-SAS (V), D, L on

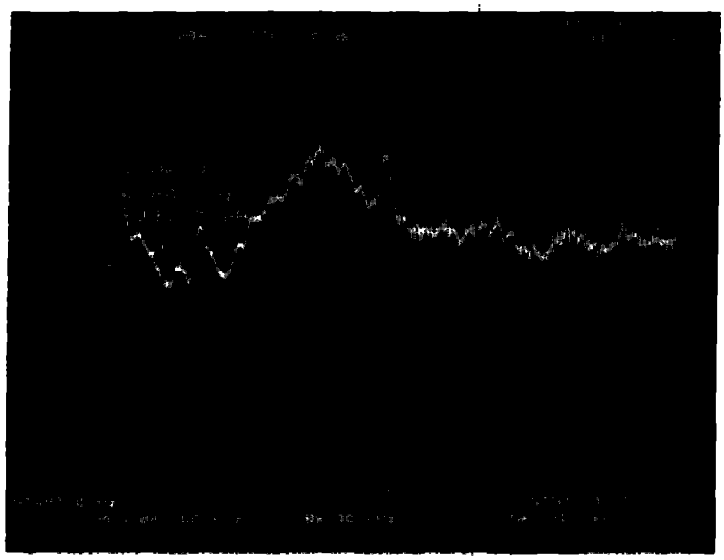

Ref. -10 dBm
Atten. 10 dB
Scale. 10 dB/Div.
Freq. 0-10 MHz

Fig. 18 Plt-SAS (V), D, L on

Ref. 0 dBm
Atten. 10 dB
Scale. 10 dB/Div.
Freq. 0-100 MHz

Fig. 19 Plt-SAS (V), D, L on

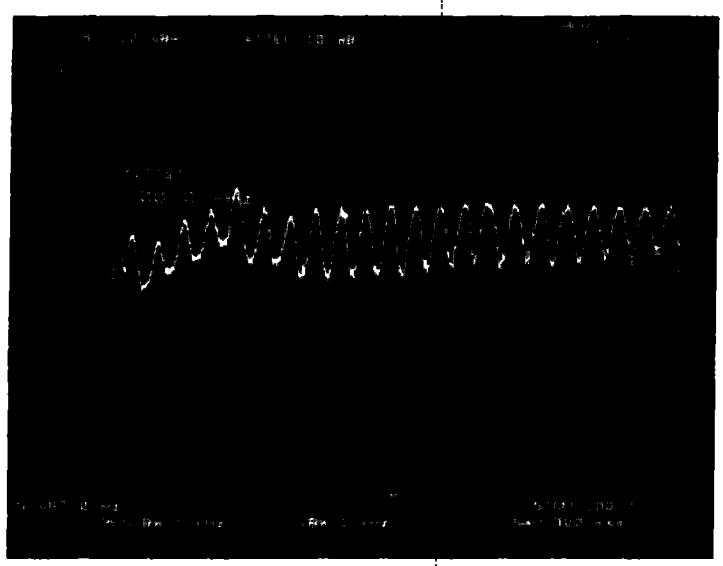

Ref. 0 dBm
Atten. 10 dB
Scale. 10 dB/Div.
Freq. 0-0.1 MHz

Fig. 20 PR-SAS (V), D, L on

Ref. 0 dBm
Atten. 10 dB
Scale. 10 dB/Div.
Freq. 0-100 MHz

Fig. 21 PR-SAS (V), D, L on

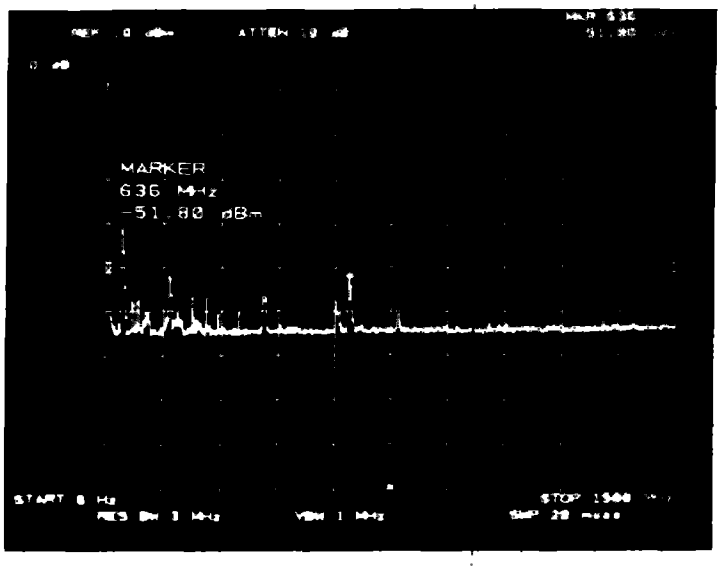

Ref. 0 dBm
Atten. 10 dB
Scale. 10 dB/Div.
Freq. 0-1500 MHz

Fig. 22 PR-SAS (V), D, L on

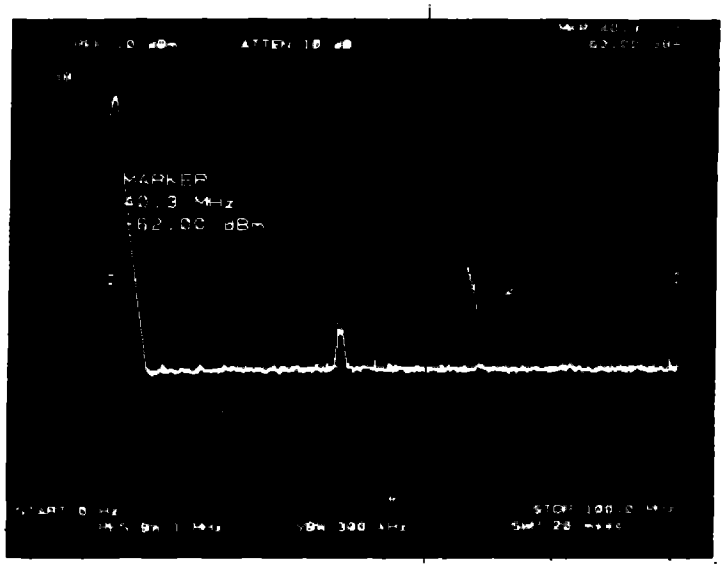

Ref. 0 dBm
Atten. 10 dB
Scale. 10 dB/Div.
Freq. 0-100 MHz

Fig. 23 PR-D-Dot, D, L on

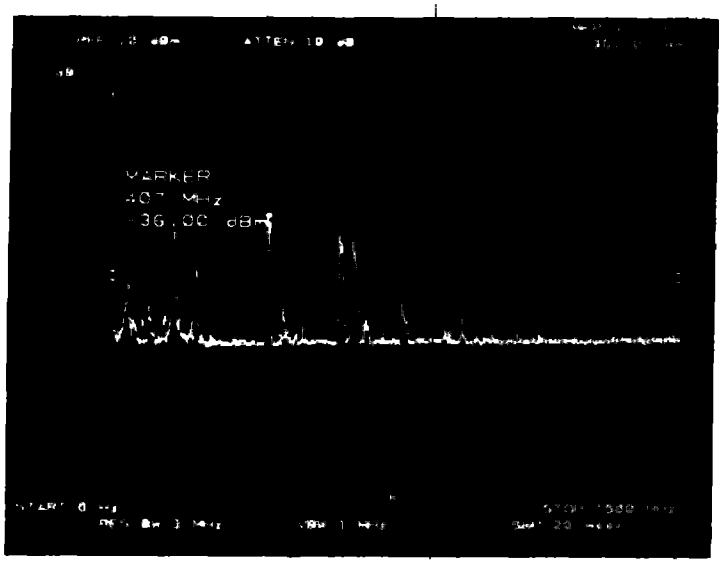

Ref. 0 dBm
Atten. 10 dB
Scale. 10 dB/Div.
Freq. 0-0.1 MHz

Fig. 24 VCR-SAS (V), D, L on

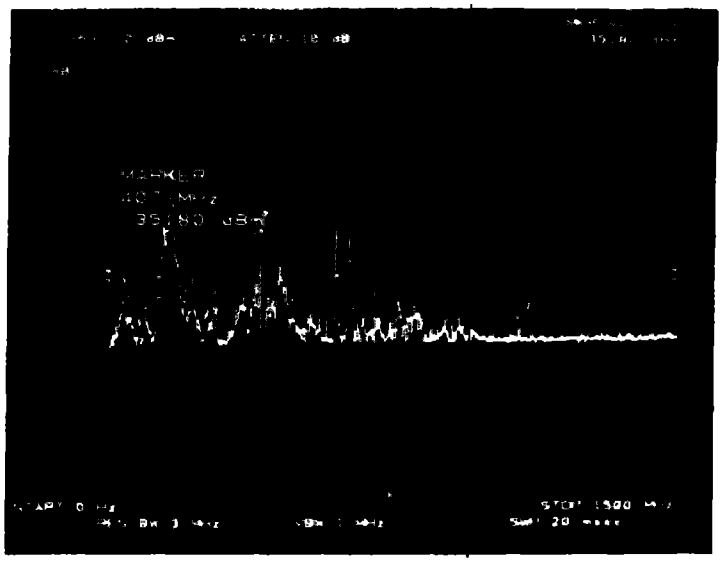

Ref. 0 dBm
Atten. 10 dB
Scale. 10 dB/Div.
Freq. 0-1500 MHz

Fig. 25 VCR-SAS (V), D, L on

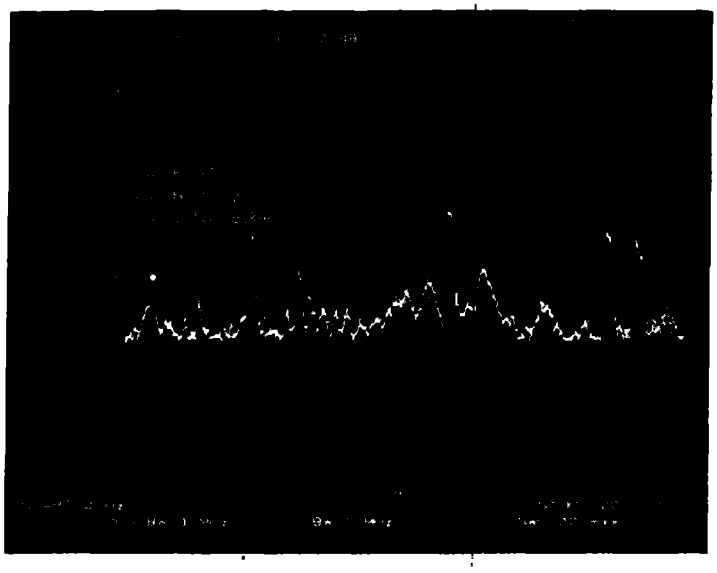

Ref. 0 dBm
Atten. 10 dB
Scale. 10 dB/Div.
Freq. 0-700 MHz

Fig. 26 VCR-SAS (V), D, L on

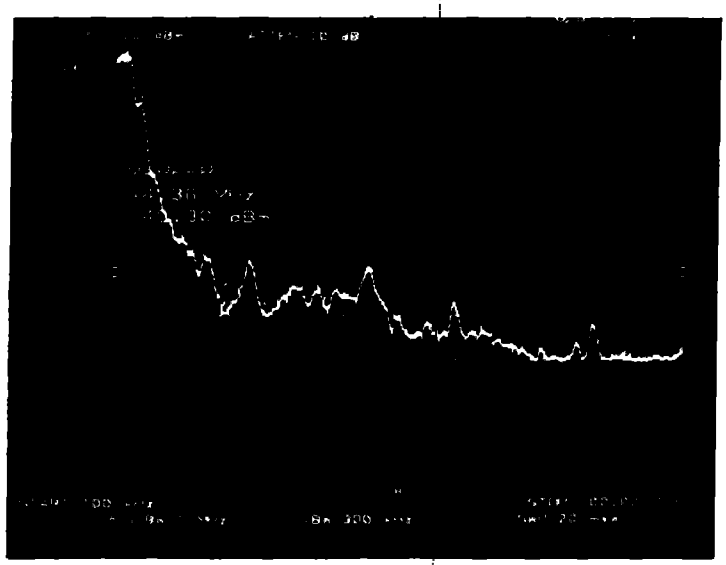

Ref. 0 dBm
Atten. 10 dB
Scale. 10 dB/Div.
Freq. 0.1-100 MHz

Fig. 27 VCR-SAS (V), D, L on

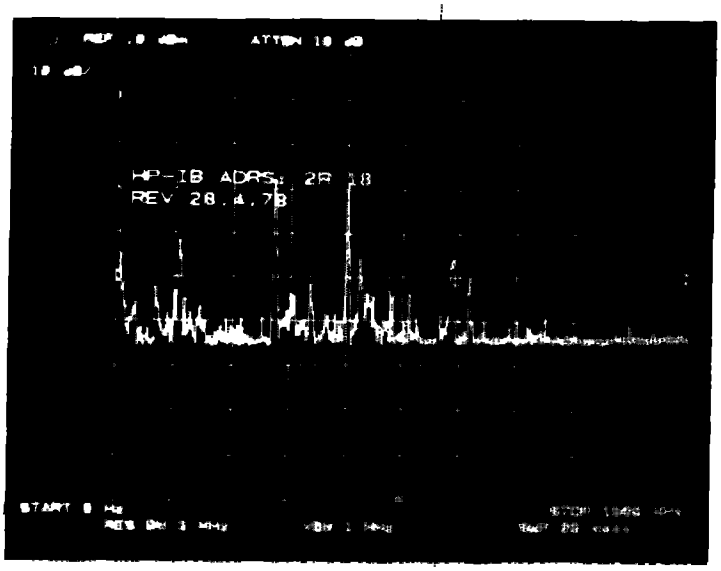

Ref. 0 dBm
Atten. 10 dB
Scale. 10 dB/Div.
Freq. 0-1500 MHz

Fig. 28 SL-SAS (V)

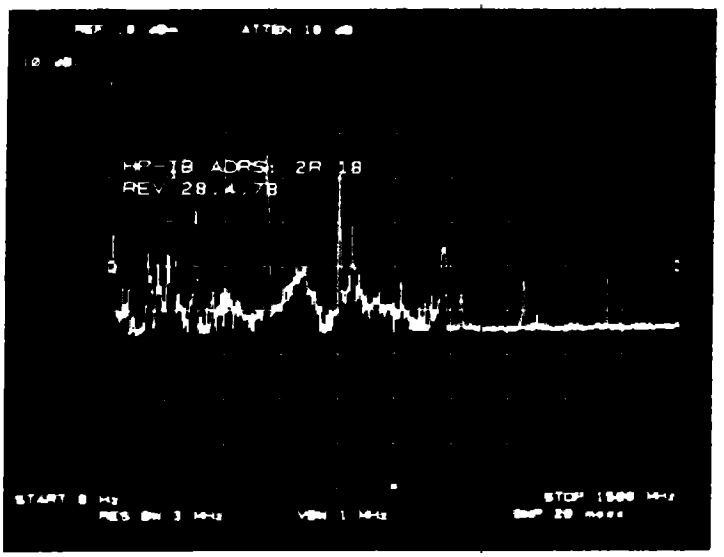

Ref. 0 dBm
Atten. 10 dB
Scale. 10 dB/Div.
Freq. 0-1500 MHz

Fig. 29 SL-SAS (V)

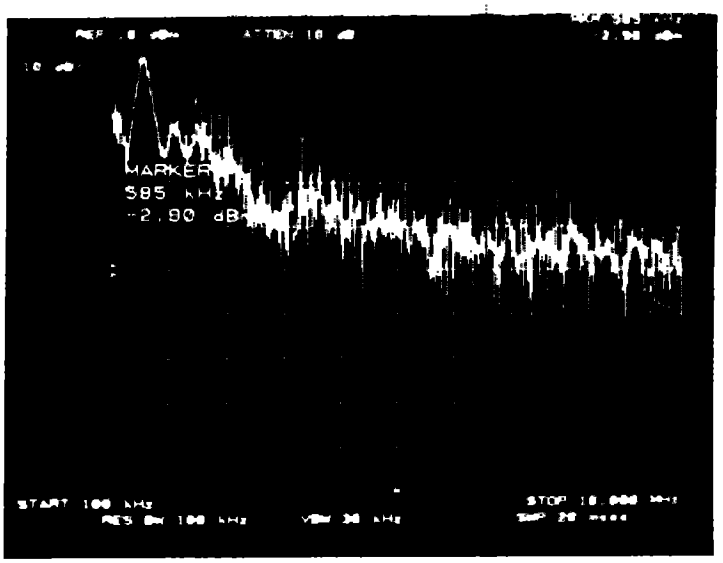

Ref. 0 dBm
Atten. 10 dB
Scale. 10 dB/Div.
Freq. 0.1-10 MHz

Fig. 30 SL-SAS (V)

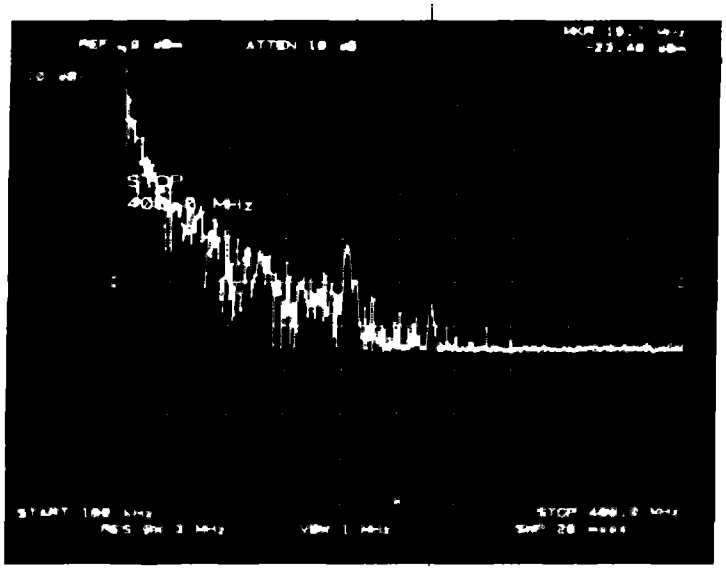

Ref. 0 dBm
Atten. 10 dB
Scale. 10 dB/Div.
Freq. 0-400 MHz

Fig. 31 SL-SAS (V)

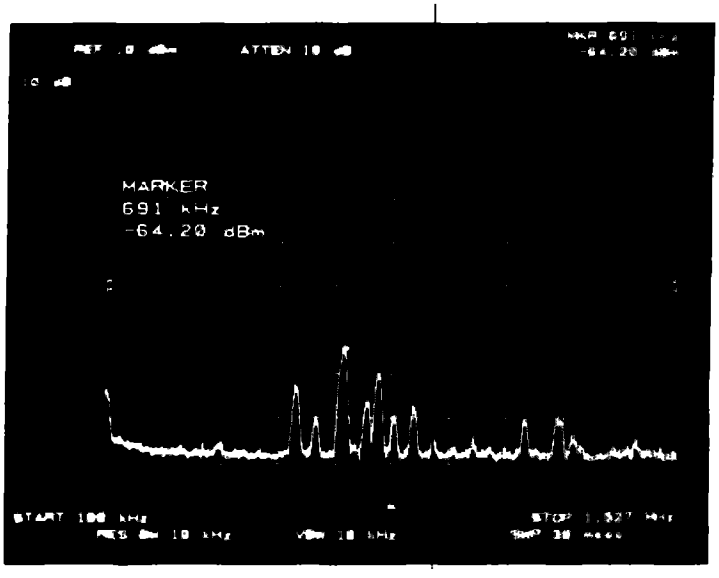

Ref. 0 dBm
Atten. 10 dB
Scale. 10 dB/Div.
Freq. 0.1-1527 MHz

Fig. 32 SL-Blue Loop

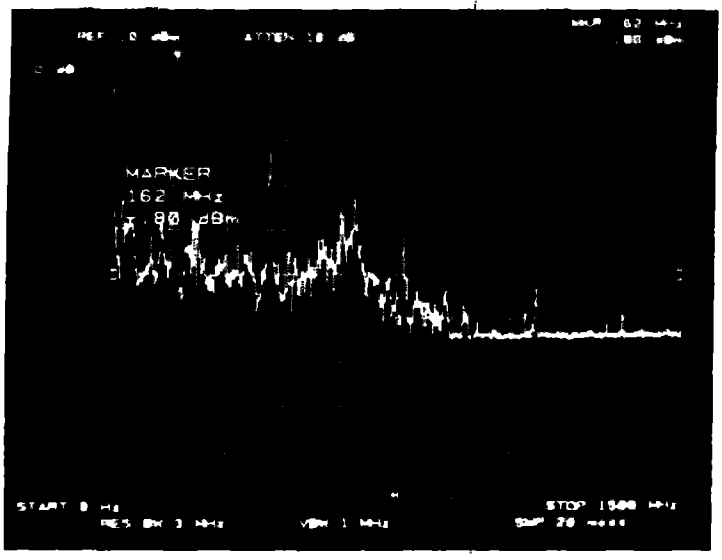

Ref. 0 dBm
Atten. 10 dB
Scale. 10 dB/Div.
Freq. 0-1500 MHz

Fig. 33 SY-SAS (V)

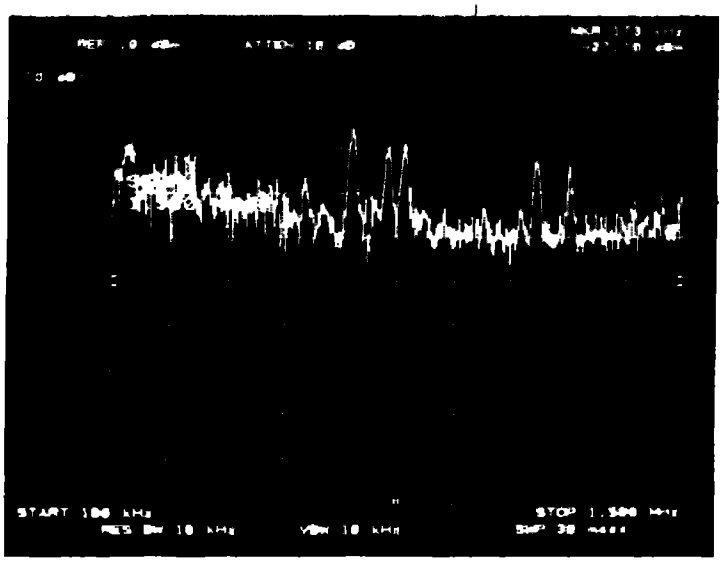

Ref. 0 dBm
Atten. 10 dB
Scale. 10 dB/Div.
Freq. 0.1-1500 MHz

Fig. 34 SY-SAS (V)

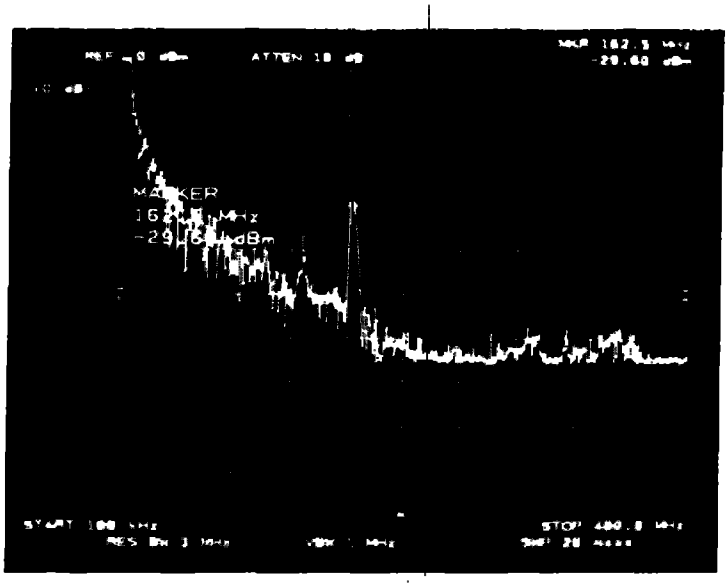

Ref. 0 dBm
Atten. 10 dB
Scale. 10 dB/Div.
Freq. 0.1-400MHz

Fig. 35 SY-SAS (V)

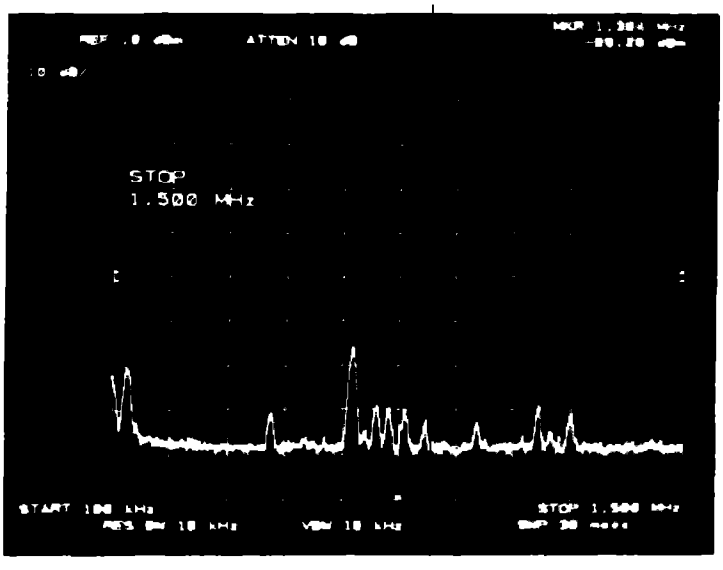

Ref. 0 dBm
Atten. 10 dB
Scale. 10 dB/Div.
Freq. 0.1-400 MHz

Fig. 36 SY-Blue Loop

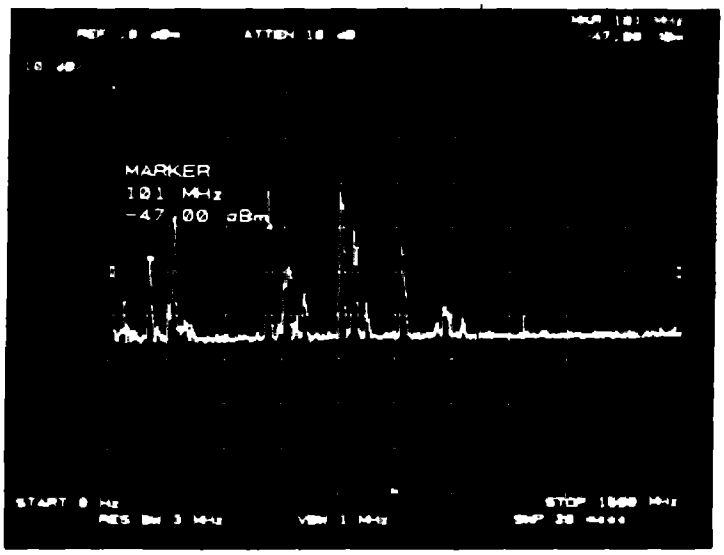

Ref. 0 dBm
Atten. 10 dB
Scale. 10 dB/Div.
Freq. 0-1500 MHz

Fig. 37 619X-SAS (V)

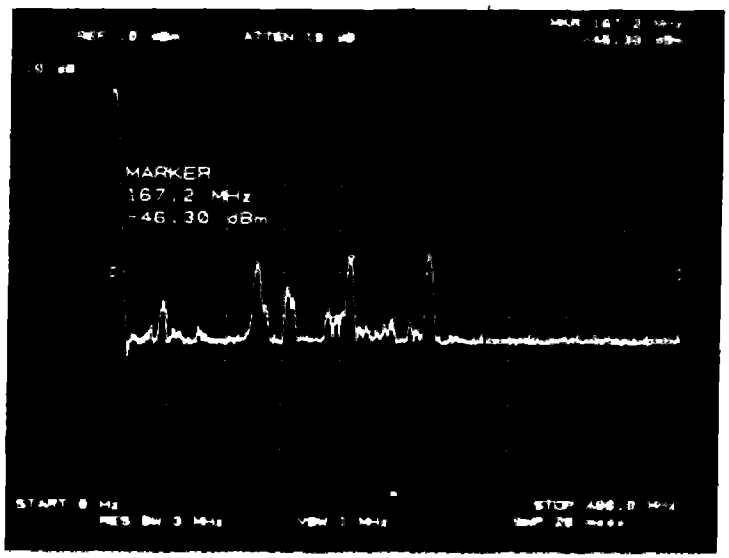

Ref. 0 dBm
Atten. 10 dB
Scale. 10 dB/Div.
Freq. 0-400 MHz

Fig. 38 619X-SAS (V)

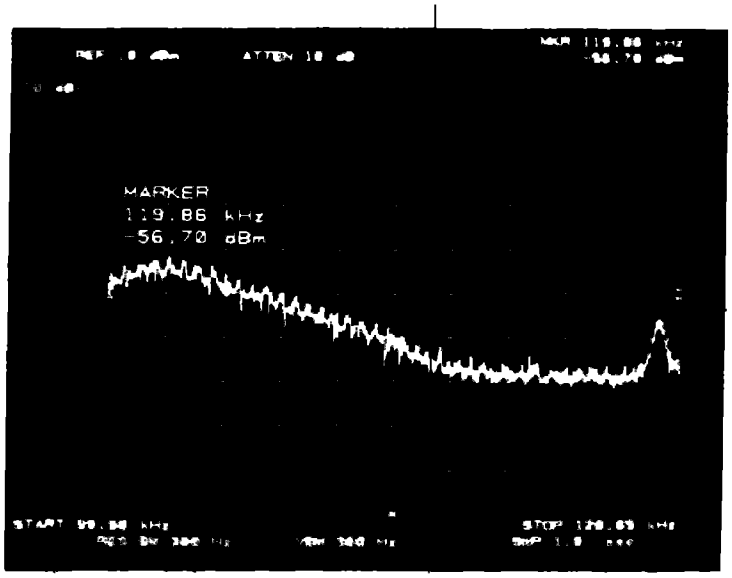

Ref. 0 dBm
Atten. 10 dB
Scale. 10 dB/Div.
Freq. 99.9-120 kHz

Fig. 39 619X-SAS (V)

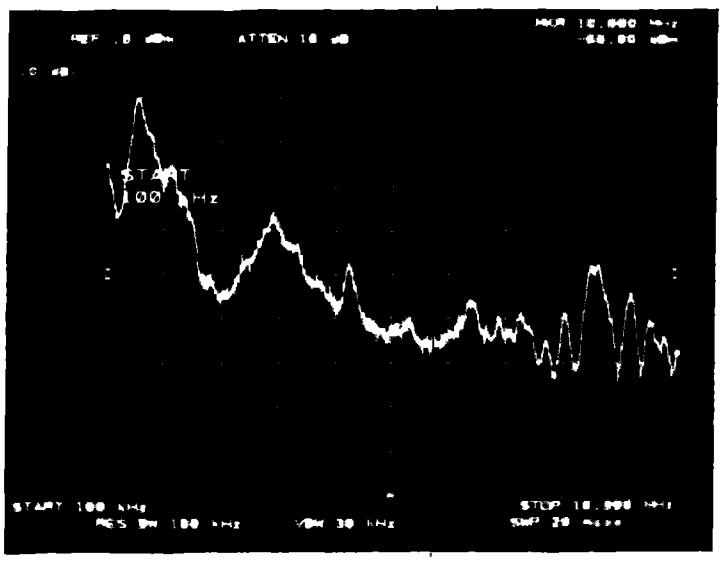

Ref. 0 dBm
Atten. 10 dB
Scale. 10 dB/Div.
Freq. 0.1-10 MHz

Fig. 40 619X-SAS (V)

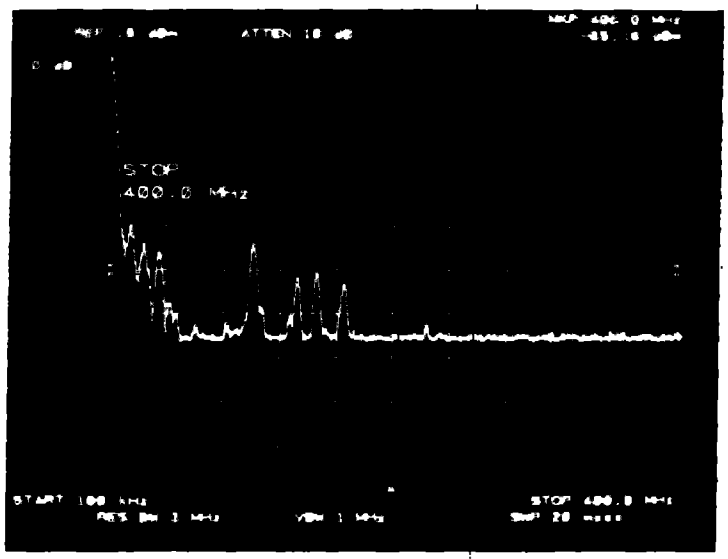

Ref. 0 dBm
Atten. 10 dB
Scale. 10 dB/Div.
Freq. 0.1-400 MHz

Fig. 41 619X-SAS (V)